

Electronic Supplementary Information

Thermal behaviour of dicarboxylic ester bithiophene polymers exhibiting a high open-circuit voltage

Ruurd Heuvel, Fallon J. M. Colberts, Martijn M. Wienk, René A. J. Janssen

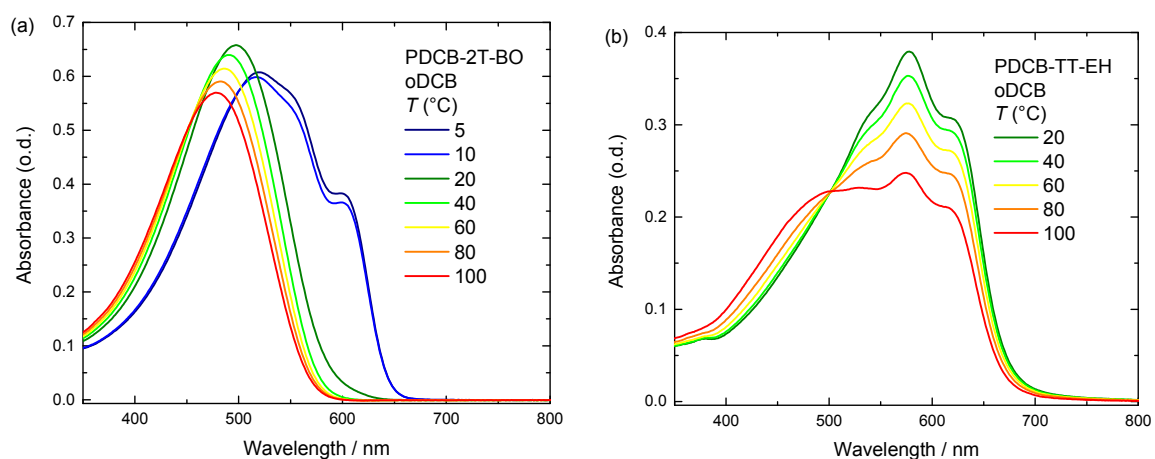


Fig. S1 Temperature dependent optical absorption spectra of (a) PDCB-2T-BO and (b) PDCB-TT-EH in oDCB.

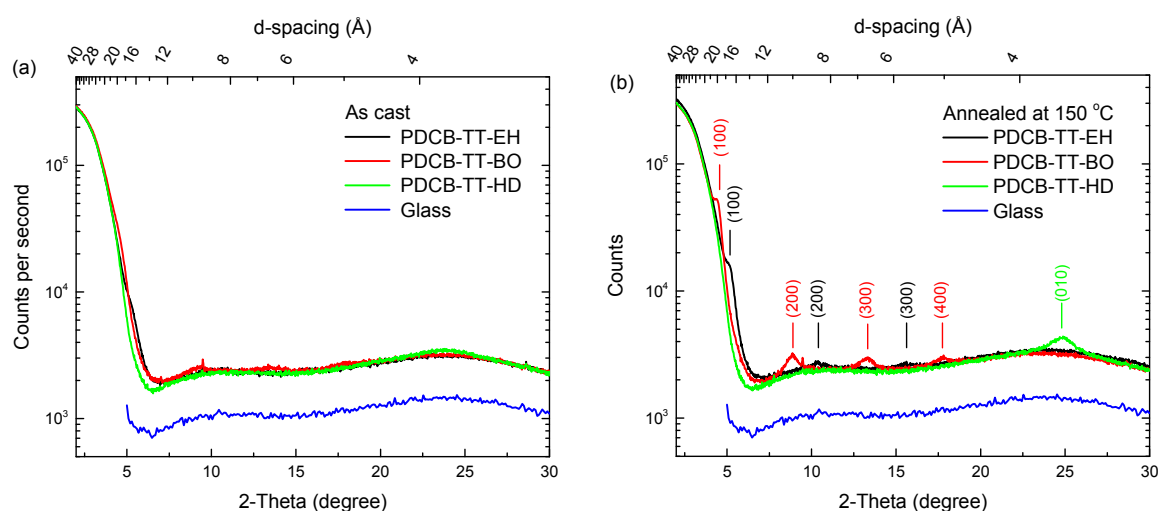


Fig. S2 X-ray diffractograms of drop cast polymer films (a) before and (b) after annealing for 30 min at 150 °C. For PDCB-TT-EH and PDCB-TT-BO lamellar spacing is seen with characteristic distance of 17.2 and 20.0 Å respectively, while for PDCB-TT-HD only a π -stacking reflection of 3.58 Å can be seen. The intensities of the reflections increase upon thermal annealing.

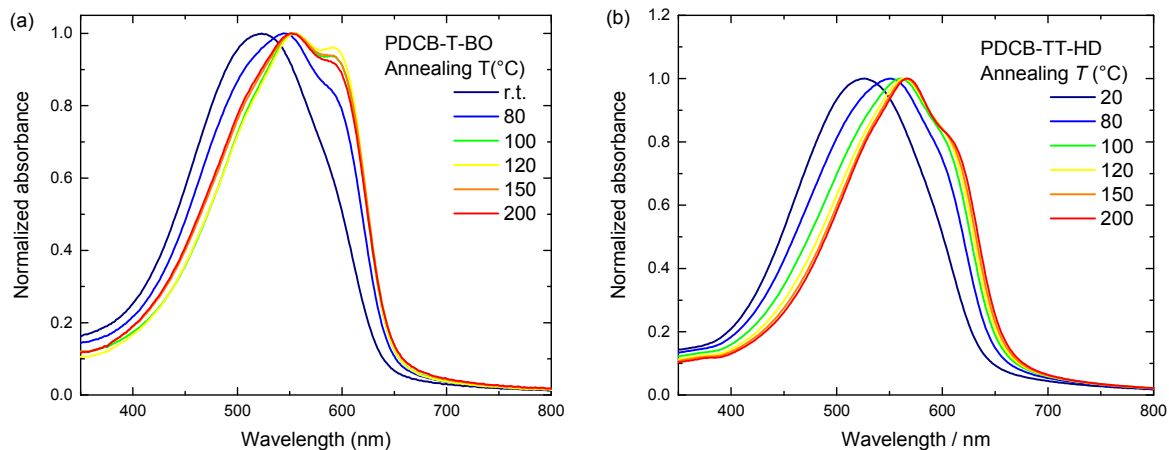


Fig. S3 Optical absorption spectra after thermal annealing of thin pristine films of (a) PDCB-T-BO and (b) PDCB-TT-HD at different temperatures for 10 min.

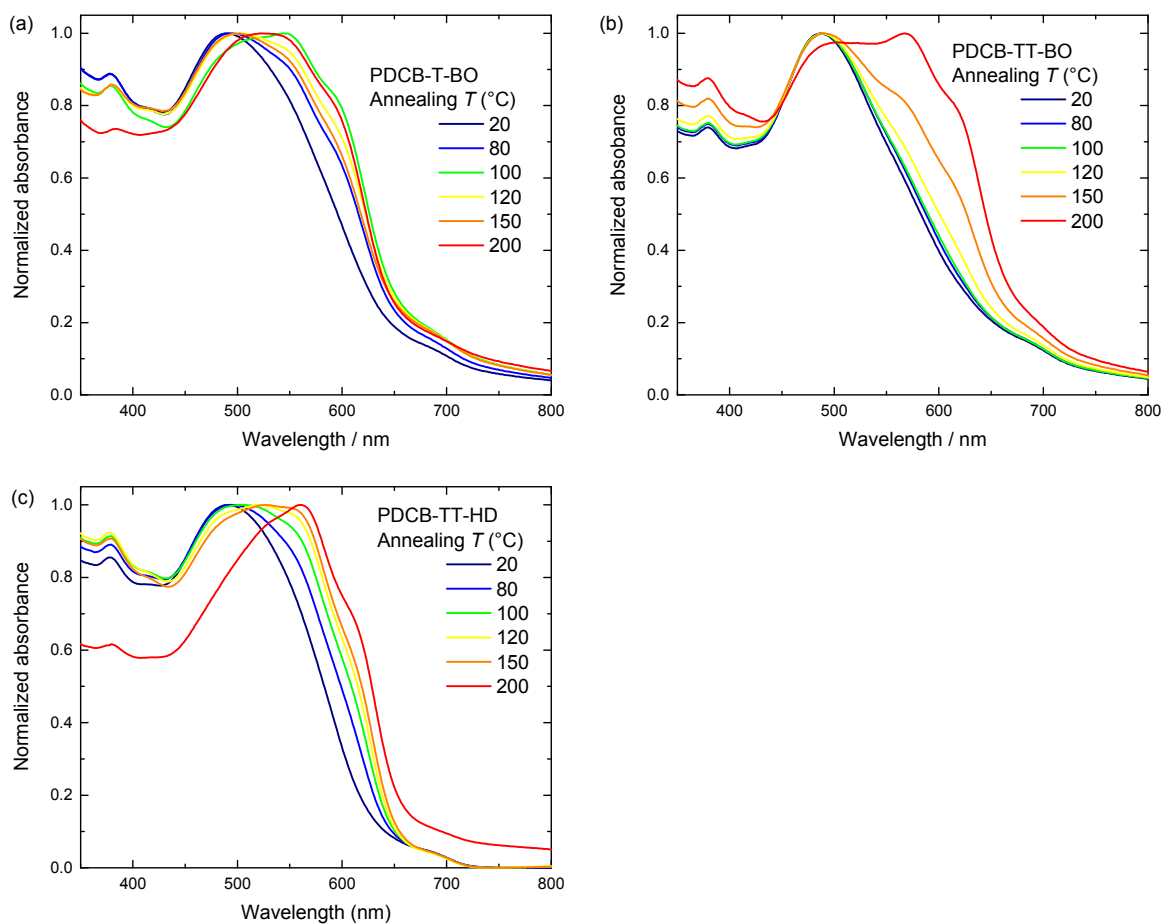


Fig. S4 Optical absorption spectra after thermal annealing at different temperatures for 10 min of PC₇₁BM blend films with (a) PDCB-T-BO; (b) PDCB-TT-BO; and (c) PDCB-TT-HD.

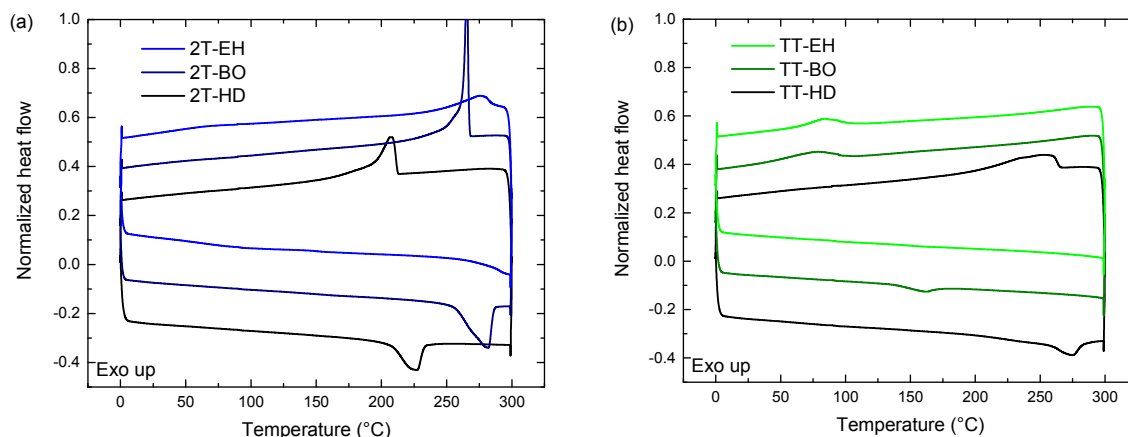


Fig. S5 Differential scanning calorimetry traces of PDCB polymers. (a) PDCB-2T and (b) PDCB-2TT. The small bumps seen for the PDCB-TT polymers could not be reproduced in other measurements.

Table S1 Optimization of photovoltaic devices using a bulk heterojunction active layer blend of PDCB polymers with PC₇₁BM cast from chloroform with different concentrations of diphenyl ether.

Polymer	DPE [vol. %]	J_{sc} [mA/cm ²]	V_{oc} [V]	FF	PCE [%]
PDCB-T-EH	0	2.99	0.97	0.55	1.60
	1	7.13	0.96	0.70	4.78
	2	7.06	0.96	0.66	4.50
	5	5.92	0.93	0.63	3.49
PDCB-2T-EH	-	-	-	-	-
PDCB-TT-EH	-	-	-	-	-
PDCB-T-BO	0	2.02	1.01	0.42	0.86
	1	2.67	0.99	0.54	1.44
	2	3.26	0.98	0.58	1.85
	5	3.21	0.99	0.60	1.92
PDCB-2T-BO	0	4.60	0.82	0.63	2.38
	1	9.88	0.74	0.71	5.19
	2	9.97	0.71	0.67	4.75
	5	9.13	0.70	0.61	3.92
PDCB-TT-BO	0	4.31	0.98	0.53	2.24
	1	6.62	0.92	0.68	4.12
	2	5.73	0.87	0.62	3.10
	5	5.51	0.89	0.63	3.07
PDCB-T-HD	0	0.55	1.02	0.49	0.28
	1	0.37	1.02	0.46	0.17
	2	0.26	1.03	0.40	0.11
	5	0.13	1.02	0.32	0.04
PDCB-2T-HD	0	3.33	0.82	0.62	1.69
	1	5.77	0.77	0.65	2.89
	2	8.19	0.74	0.64	3.87
	5	6.65	0.71	0.55	2.59
PDCB-TT-HD	0	1.78	0.94	0.56	0.94
	1	4.71	0.91	0.54	2.30
	2	6.07	0.87	0.48	2.53
	5	5.13	0.84	0.43	1.87

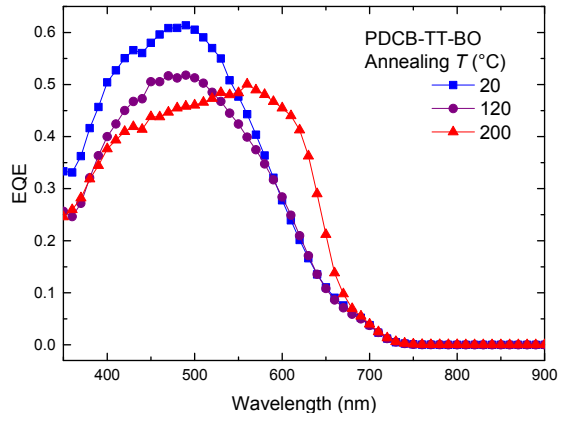


Fig. S6 EQE spectra of optimized bulk heterojunction solar cells of PDCB-TT-BO after temperature dependent annealing.

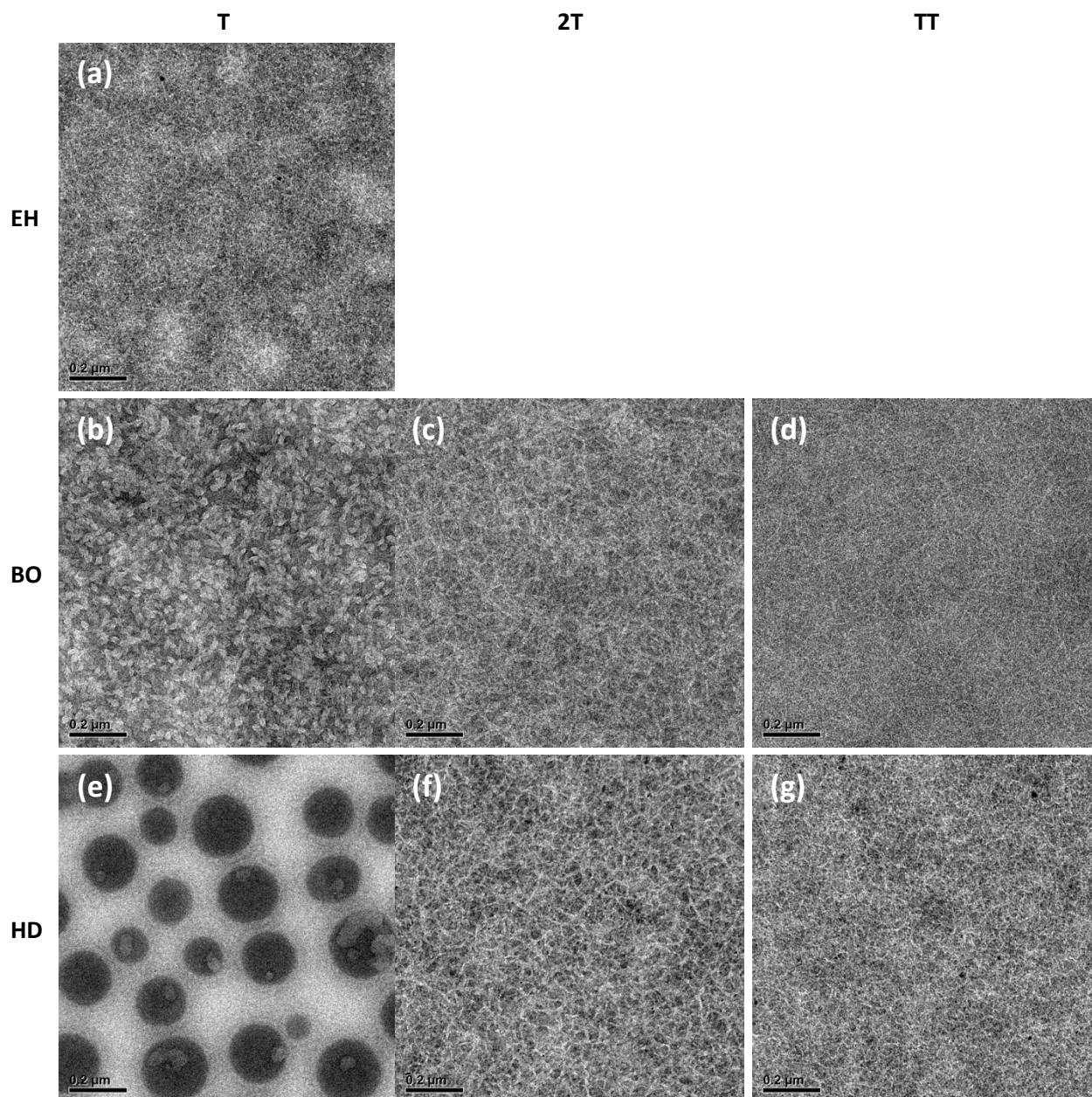


Fig. S7 Bright-field TEM micrographs of optimized, pristine active layer PC₇₁BM blends with PDCB polymers (a) T-EH; (b), T-BO; (c), 2T-BO; (d), TT-BO; (e), T-HD; (f) 2T-HD; (g) and TT-HD. Scale bars are 200 nm.

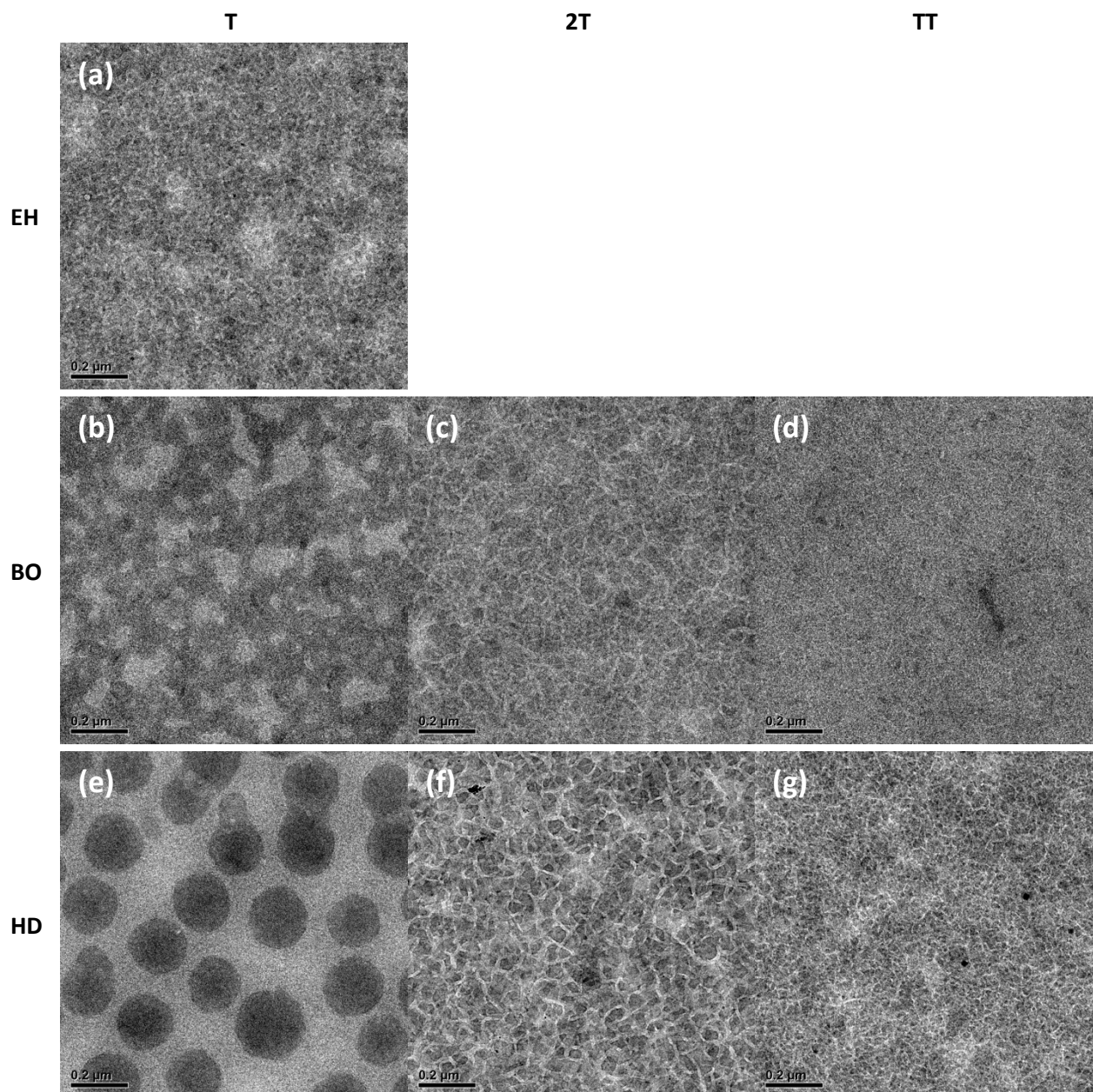


Fig. S8 Bright-field TEM micrographs of optimized and thermally annealed active layer PC₇₁BM blends with PDCB polymers (a) T-EH; (b), T-BO; (c), 2T-BO; (d), TT-BO; (e), T-HD; (f) 2T-HD; (g) and TT-HD. Scale bars are 200 nm.

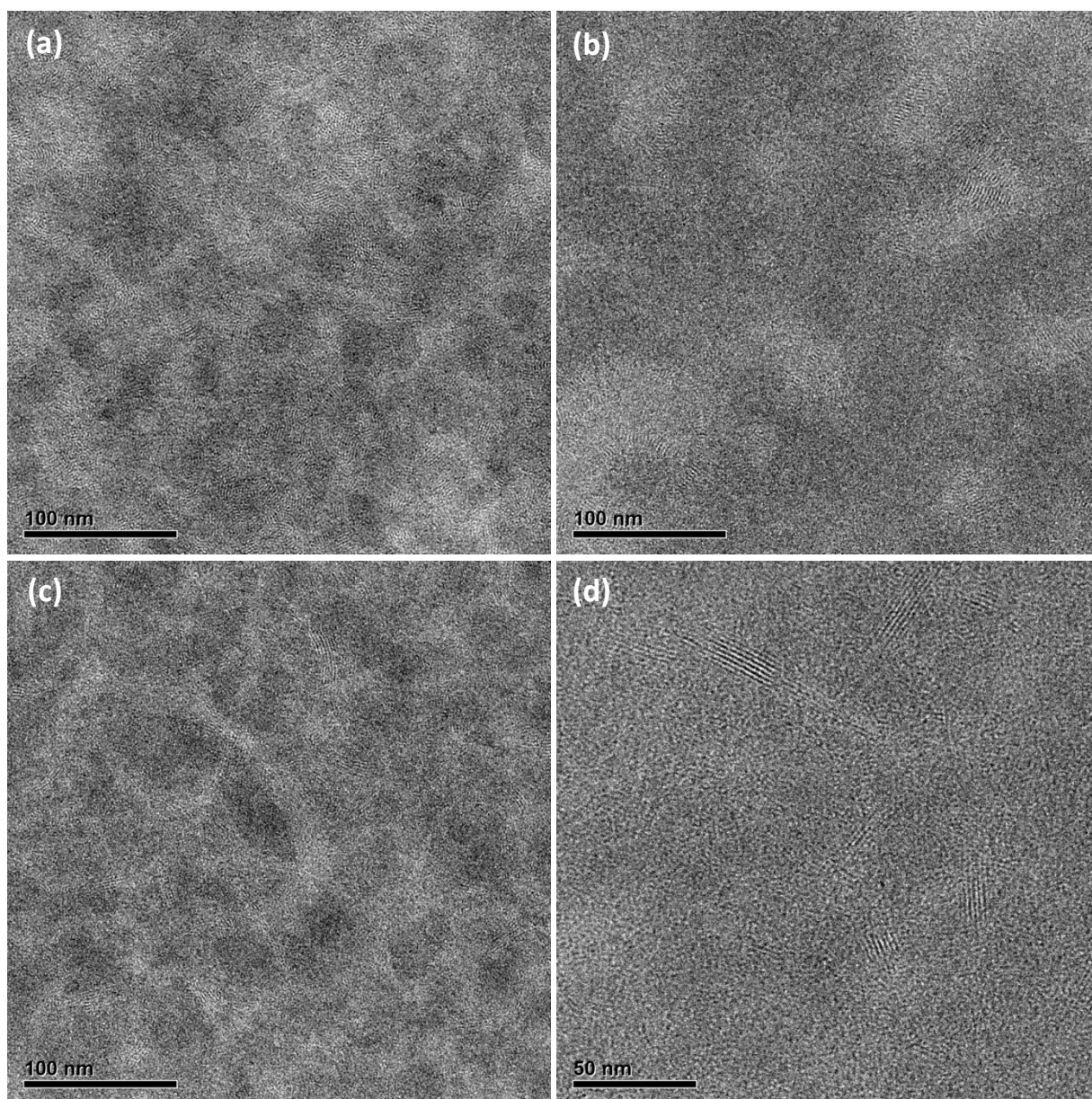


Fig. S9 Zoomed in bright-field TEM micrographs of optimized active layer PC₇₁BM blends with (a) PDCB-T-EH after thermal annealing; (b) PDCB-T-BO after thermal annealing; (c) PDCB-2T-BO (pristine); (d) PDCB-TT-BO (pristine). In each case crystal lattice fringes present in selected areas of the film indicate the semi-crystalline nature of the polymer phase. Scale bars are 100 nm (a-c) and 50 nm (d).

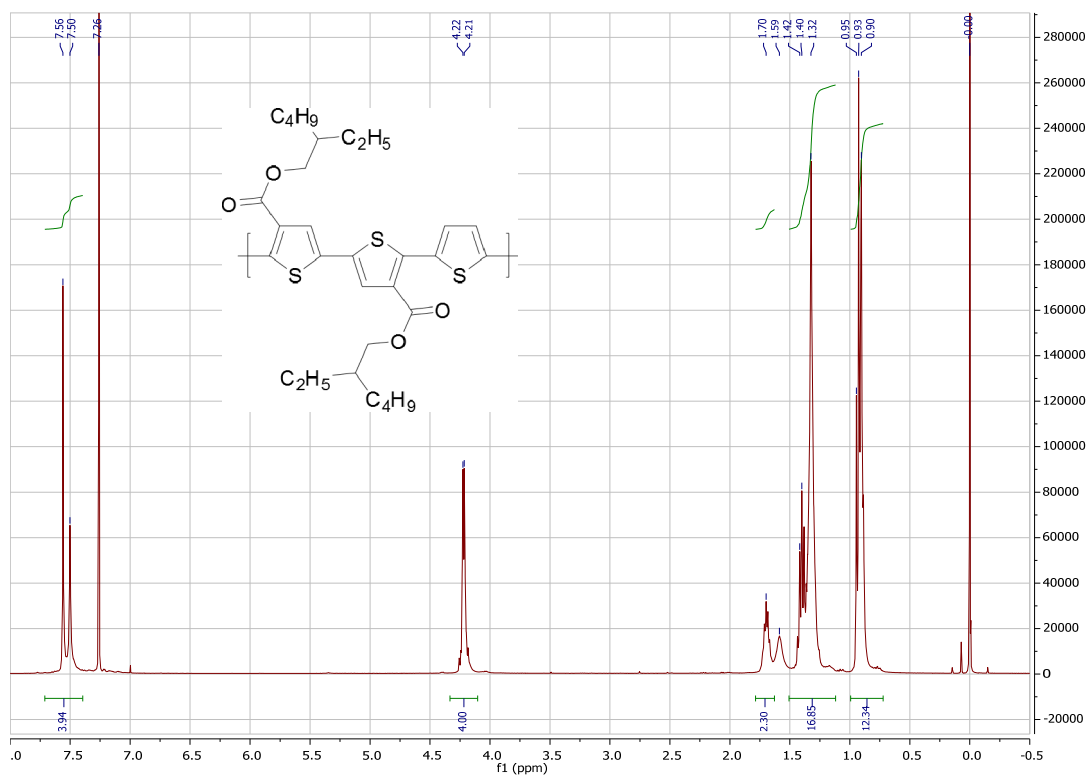


Fig. S10 ^1H NMR spectrum of PDCB-T-EH

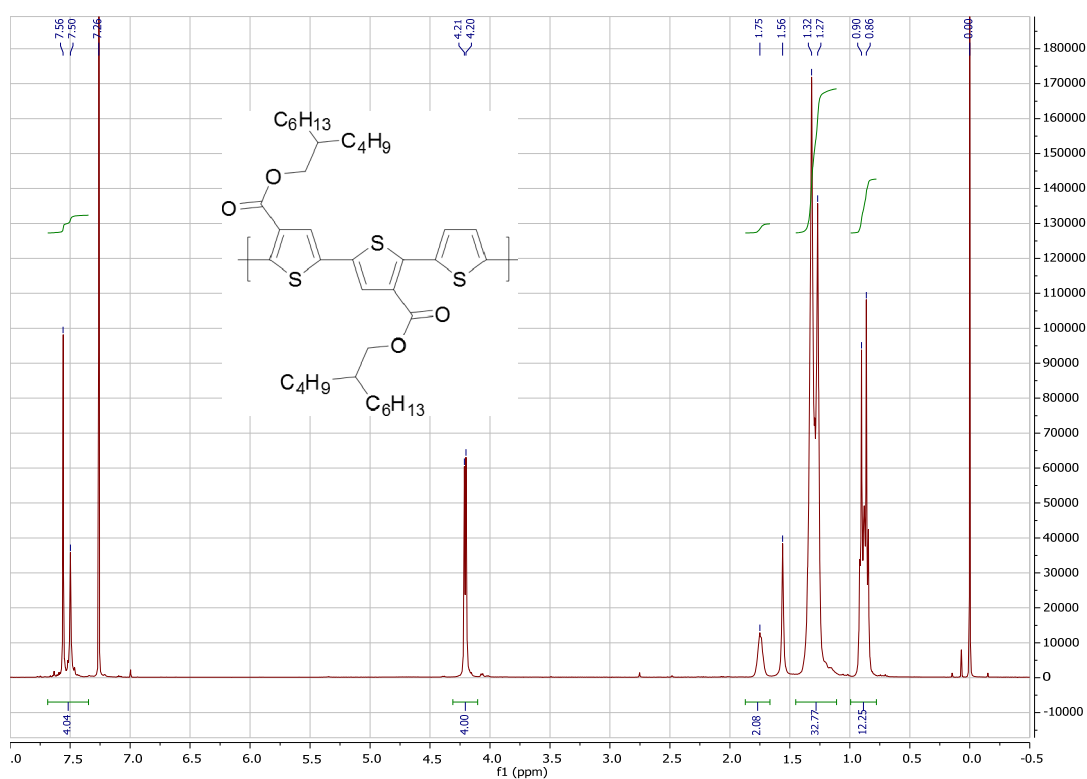


Fig. S11 ^1H NMR spectrum of PDCB-T-BO

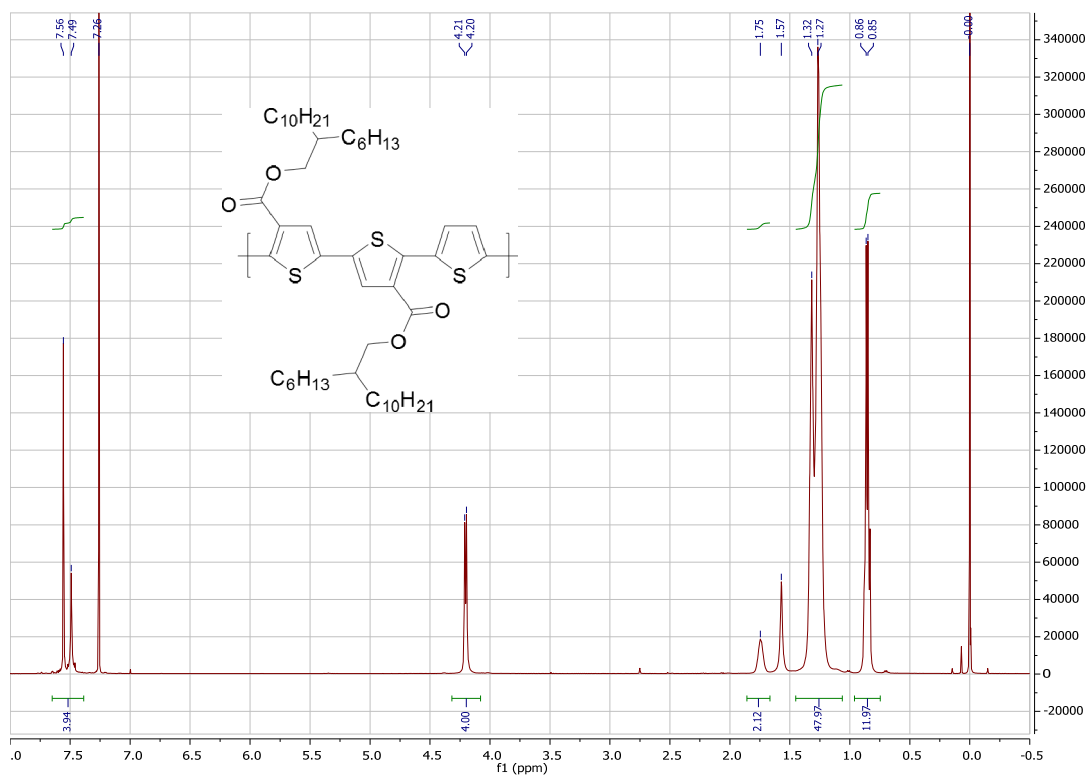


Fig. S12 ^1H NMR spectrum of PDCB-T-HD

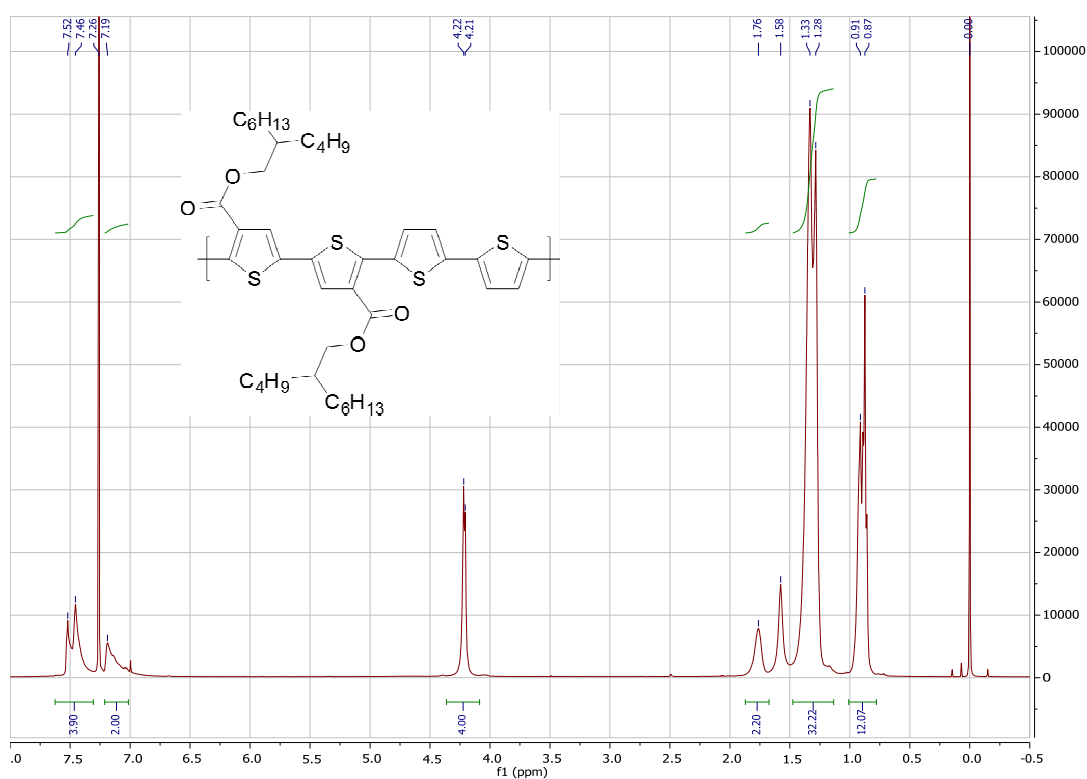


Fig. S13 ^1H NMR spectrum of PDCB-2T-BO

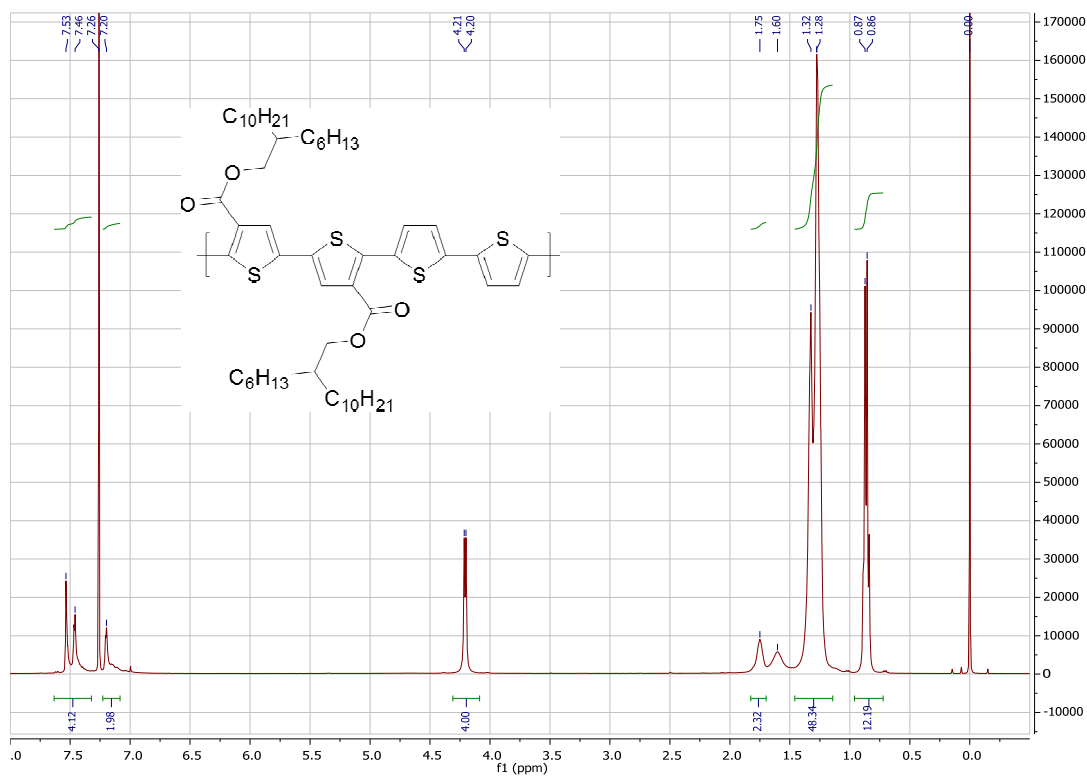


Fig. S14 ¹H NMR spectrum of PDCB-2T-HD

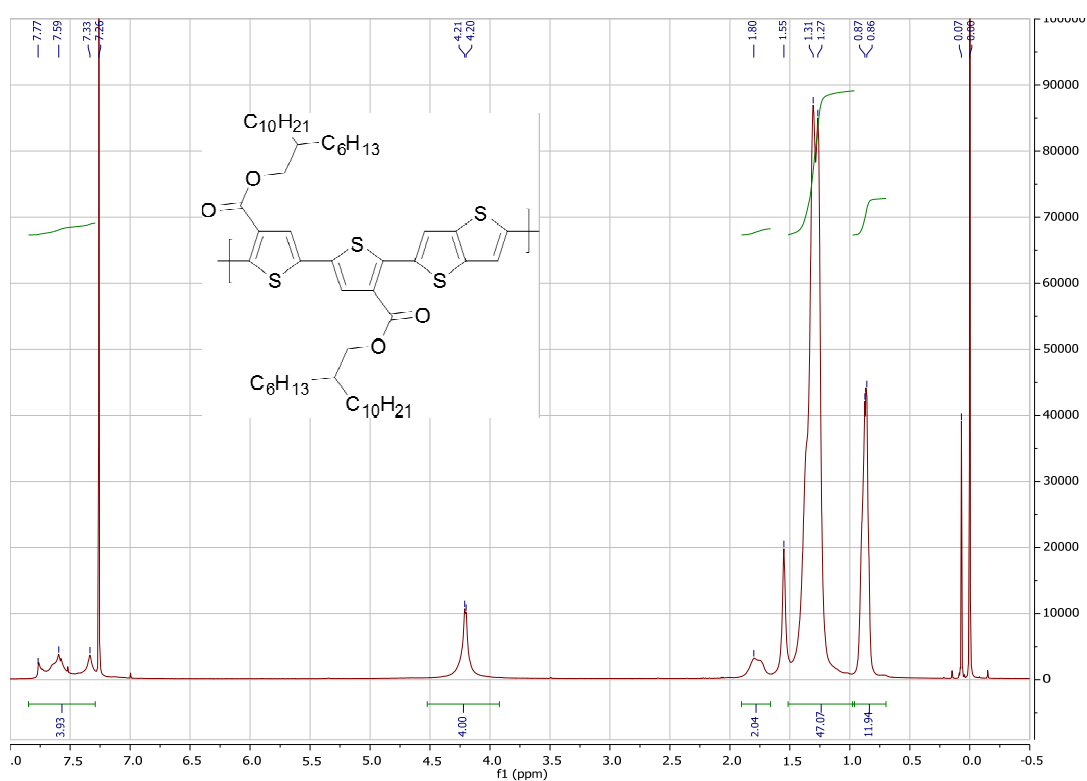


Fig. S15 ¹H NMR spectrum of PDCB-TT-HD